Field Experiments and Predicting using C-LSTM Networks of Bridge Position Estimation

Shin Ryota, Yamamoto Kyosuke, Okada Yukihiko

***Abstract*— In this study, a bridge position determination technique was validated using real-world data. The results can visually judge the location of some bridges. We also performed supervised binary classification for bridge location estimation using C-LSTM. Although the accuracy is not high, it is possible to estimate the approximate location of the bridge.**

***Index Terms*—on-going monitoring, VBI system, CNN, LSTM**

I. Introduction

Bridges play an essential role in the transportation system. However, it is not efficient to perform maintenance and inspection of a large number of bridges uniformly. Therefore, we decided to prioritize the inspection of bridges with a high possibility of damage after conducting a simple screening in advance. To achieve this, the condition of the bridges needs to be easily and quickly understood.

As a way to do this, vibration-based monitoring methods are being considered. They fall into two categories. The first is "direct bridge monitoring technology," in which sensors are installed on the bridge. Although this method can monitor the bridge's condition with high accuracy, it is time-consuming and costly because it requires the installation of multiple sensors on a single bridge. Besides, even if we build a system to monitor a bridge's condition from the acceleration data obtained, it is not easy to apply it to other bridges. The second approach is an indirect bridge monitoring technique, in which sensors are installed only on vehicles. Yang et al. [1] proposed a vehicle response analysis to estimate a bridge's vibration from the vibration obtained when a vehicle equipped with an accelerometer runs over the bridge. Recent studies on vehicle response analysis include estimation of natural frequencies of bridges [2], damage detection [3, 4], and position estimation [5].

However, there are challenges in socially implementing a bridge monitoring system using vehicle response analysis. One of the challenges in socially implementing a bridge monitoring system using vehicle response analysis is to identify the bridge's location from the vehicle vibration data. In most of the previous studies, only the data on the bridge was analyzed. Therefore, the technology to extract only the bridge part from the vehicle acceleration data is one of the technical challenges for the social implementation of vehicle response analysis.

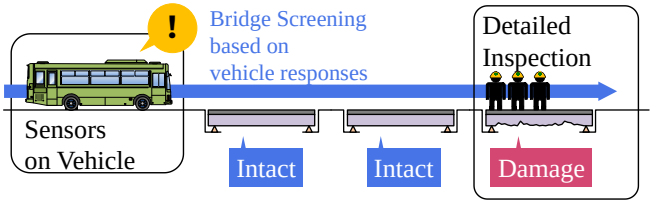

Fig. 1 Conceptual Diagram of Bridge Screening

Murai et al. [5] have verified the bridge position estimation from vehicle vibration data by numerical simulation. Acceleration sensors are installed in the unsprung masses of the front and rear axles. The paper shows that the bridge can be detected by synchronizing and subtracting two-vehicle vibration data in the spatial domain using GPS data. This is based on the vehicle-bridge interaction (VBI) when a vehicle travels over a bridge. The effect of noise has also been studied. As noise increases, the difference between the acceleration data obtained on the bridge and the acceleration data obtained on the road becomes smaller. It is pointed out that it is impossible or difficult to determine the bridge's response from the measured data because the data obtained from field experiments contain various noises. Therefore, the selection of vibration waveforms requires personnel and incurs new costs, which is not desirable.

In recent years, deep learning has been widely used in image recognition and signal processing [6]. There are two main types of deep learning methods: convolutional neural networks (CNN) used for image recognition and recurrent neural networks (RNN) mainly used for natural language processing and speech recognition. CNN can learn local responses from spatial and temporal data, but they cannot learn sequential correlations. On the other hand, RNNs are characterized by sequential modeling, but they are not suitable for parallel processing [7]. To deal with gradient explosion and disappearance that occurs in general RNNs, we introduce the Long Short-Term Memory (LSTM) unit. This enables analysis, including past information [8]. Zhou et al. [9] proposed C-LSTM, which combines CNN and LSTM to learn temporal and spatial features. Various researches have been conducted using this model, such as prediction [8] and anomaly detection [6] in data with temporal and spatial features. Acceleration data of a vehicle passing over a bridge

Manuscript received March 23, 2020; revised April 24, 2021. This work was partly supported by JSPS KAKENHI Grant Number 19H02220 (Grant-in-Aid for Scientific Research(B)).

Shin Ryota is a master student of University of Tsukuba, Ibaraki prefecture, Japan (e-mail: s1920556@s.tsukuba.ac.jp).

Yamamoto Kyosuke is an assistant professor of University of Tsukuba, Ibaraki, Japan (e-mail: yamamoto_k@kz.tsukuba.ac.jp).

Okada Yukihiko is an associate professor of University of Tsukuba, Ibaraki, Japan (e-mail: okayu@sk.tsukuba.ac.jp).

ISBN: 978-988-14049-2-3
ISSN: 2078-0958 (Print); ISSN: 2078-0966 (Online)

is time-series data containing temporal and spatial features. Therefore, we thought that by using C-LSTM, we could create a model that can distinguish only the part of the vehicle running on the bridge from the vehicle's acceleration data.

Therefore, we decided to focus on two things: first, to validate the bridge location estimation technique in field experiments. Murai et al. [5] have validated bridge position estimation with numerical simulations, but not with field experiments. The second is developing a technique to extract only the part of the vehicle running on the bridge from the vehicle acceleration data using C-LSTM. If these are realized, it is expected that the social implementation of bridge monitoring technology using vehicle response analysis will become more realistic.

II. Method/Basic Theory

A. C-LSTM neural networks

The combination of CNN and LSTM has been studied to obtain spatial and temporal features [9]. The schematic diagram of C-LSTM is shown in Figure 2. This study's C-LSTM model is based on Kim and Cho [6] and Kim and Cho [8] and consists of Convolution, Activation, Pooling, LSTM, and Dense. Kernel size, stride size, and activation function were adjusted to minimize the loss function's value calculated from the learning data. The resulting model is presented in Table 1. CNN has two layers: a Convolution layer and a Pooling layer. The LSTM has 64 units, and the Dense layer has 32 units selected.

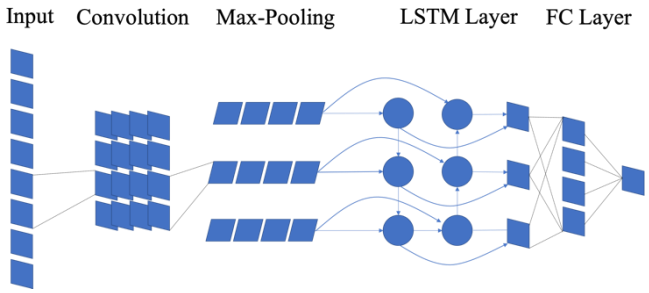

Fig. 2 Conceptual Image of C-LSTM

Table 1
The C-LSTM Architecture

Type	Kernel size	Stride	Param.
Convolusion	2×1	1	192
Activation(relu)	-	-	0
Pooling	2×1	2	0
Convolusion	2×1	1	8,256
Activation(relu)	-	-	0
Pooling	2×1	2	0
LSTM(64)	-	-	180,480
Activation(relu)	-	-	0
Dence(32)	-	-	2,080
Dence(1)	-	-	33
Activation(softmax)	-	-	0

B. Signal processing for vehicle vibration

VBI is the contact force and the bridge vibrations under the vehicle axes. When a vehicle enters a bridge, the vehicle shakes the bridge, and the bridge shakes the vehicle. The vehicle vibration is also excited by road surface unevenness. Only the bridge response is obtained when the vehicle vibration data is taken, and the bridge position is discriminated by using it in Murai et al. [5]. Fig. 3 shows a conceptual diagram of VBI occurring when a vehicle is traveling on a bridge, and Fig. 4 shows a conceptual diagram of VBI occurring when a vehicle is passing on a road.

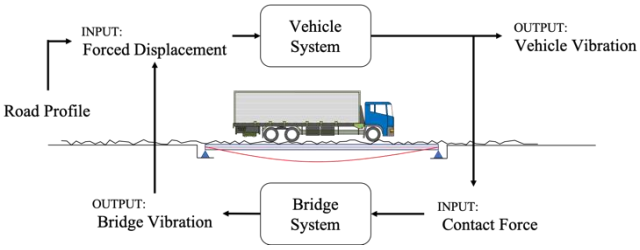

Fig. 3 Conceptual Image of VBI on the bridge

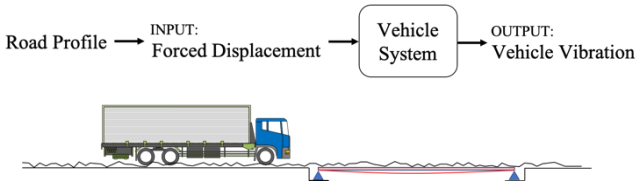

Fig. 4 Conceptual Image on the road

Table 2
Extracted Features

Feature	Equation
Maximum Value	$f_{1i} = \max(X(i))$
Mean Value	$f_{2i} = \frac{1}{N}\sum_{i=1}^{N} X(i)$
Minimum Value	$f_{3i} = \min(X(i))$
Standard Value	$f_{4i} = \sqrt{\frac{1}{N}\sum_{i=1}^{N}(X(i) - f_{1i})^2}$
Peak to Peak Value	$f_{5i} = f_{1i} - f_{3i}$
Mean Amplitude	$f_{6i} = \frac{1}{N}\sum_{i=1}^{N} \lvert X(i)\rvert$
Root Mean Square Value	$f_{7i} = \sqrt{\frac{1}{N}\sum_{i=1}^{N} X(i)^2}$
Skewness Value	$f_{8i} = \frac{1}{N}\sum_{i=1}^{N} X(i)^3$
Kurtosis Value	$f_{9i} = \frac{1}{N}\sum_{i=1}^{N} X(i)^4$
Waveform Value	$f_{10i} = \frac{f_{7i}}{f_{6i}}$
Pulse Indicator	$f_{11i} = \frac{f_{1i}}{f_{6i}}$
Kurosis Index	$f_{12i} = \frac{f_{9i}}{f_{7i}}$
Peak Index	$f_{13i} = \frac{f_{1i}}{f_{7i}}$
Square Root Amplitude	$f_{14i} = \left(\frac{1}{N}\sum_{i=1}^{N}\sqrt{\lvert X(i)\rvert}\right)^2$
Margin Indicator	$f_{15i} = \frac{f_{1i}}{f_{14i}}$
Skewness Indicator	$f_{16i} = \frac{f_{8i}}{f_{7i}^4}$

ISBN: 978-988-14049-2-3
ISSN: 2078-0958 (Print); ISSN: 2078-0966 (Online)

In this study, accelerometers were installed unsprung-mass of the front and rear wheels of the vehicle. This is because the vibration component of the high frequency of road surface and bridge can be measured directly. The obtained acceleration data are subjected to position synchronization and subtracted in a space region. As a result, the unevenness of the road surface included in the measurement data can be reduced. The experimental data were then normalized using Eq (1) before being input to C-LSTM.

$$x' = \frac{x - x_{min}}{x_{max} - x_{min}} \tag{1}$$

Then, to reduce the computation time of C-LSTM, the feature quantities used by Jiang et al. [10] are calculated. A table summarizing the feature values used is shown in Table 2. The respective feature values were calculated for each 1 step with a window size of 1000.

III. Field Experiments

A. Experimental Settings

Field experiments were conducted on the Tomei Expressway. Trucks used for essential delivery services in Japan were used as test vehicles, and accelerometers were installed unsprung-mass of the front and rear wheels for measurement. The sampling rate of the accelerometer was 300 Hz. The test truck has two axes at the front and one at the rear before the front are treated as one axis. GPS sensors were introduced to synchronize the vehicle position with the front and rear wheel positions. In this study, the acceleration data of nine bridges were measured. The data of passing on each bridge are used. The bridge position in each acceleration data was confirmed by the author and labeled. A label of 1 was given on the bridge, and 0 was given on the road. The target section of the acceleration data was determined for each bridge. The bridge's length and the road before and after the bridge were twice the lengths of the bridge. The maximum speed and minimum speed in the section were about 85.1 km/h and about 68.8 km/h, and the average speed was about 77.2 km/h. The total number of data finally obtained is 162,695, and it consists of 9 different files. The bridge part is 45,627 of them. For each file, 16 feature values were calculated with a window size of 1000, and the number of analysis data was 39,343,600.

B. The results and discussions of field experiments

Unlike numerical experiments, the spacing of data points in the spatial domain is different because the vehicle speed is not constant [2]. Therefore, the acceleration data measured unsprung-mass of the front wheels and the rear wheels are interpolated simultaneously. Then, the mutual correlation of the front axis's acceleration and the rear axis was obtained, and the difference was obtained at the position where the two waveforms matched most [5]. As an example of the difference after the position synchronization, acceleration data measured under the springs of the front and rear wheels near the bridge over the K River and vibration data after the position synchronization are shown in Fig. 5-6.

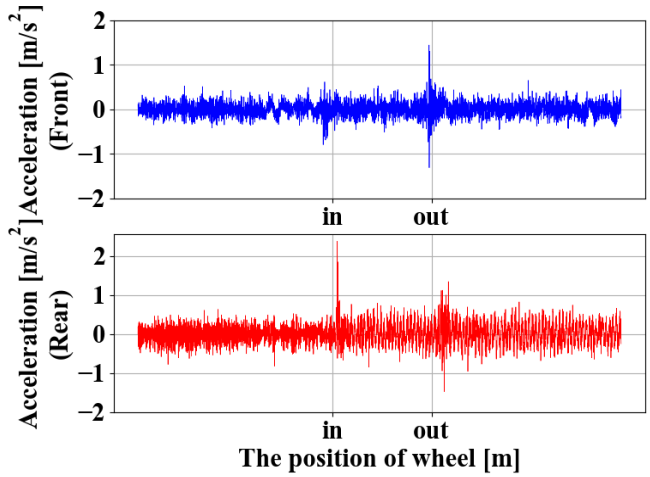

Fig. 5 Vibration data of upsprung-mass front and rear wheels measured at a bridge over the K River

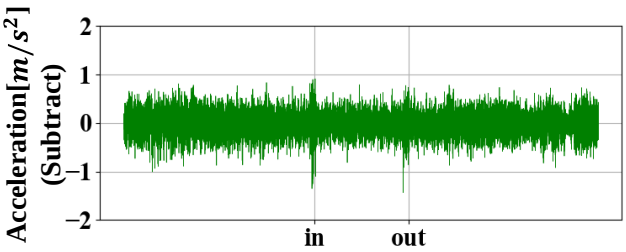

Fig. 6 Subtractions of front and rear vibration measured at a bridge over the K River

In the numerical simulation conducted by Murai et al. [5], the bridge response could be observed by taking the difference between the front and rear wheels. However, the results of this study are masked by noise and cannot be visually identified. The results for other bridges are shown in Fig. 7-9.

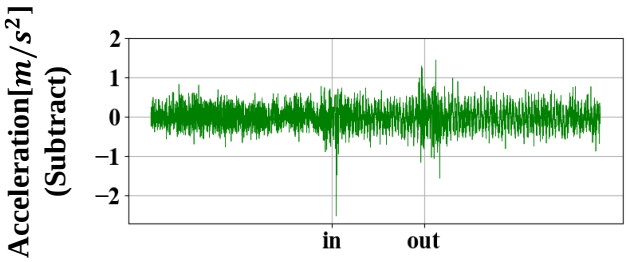

Fig. 7 Subtractions of front and rear vibration measured at a bridge over the O River

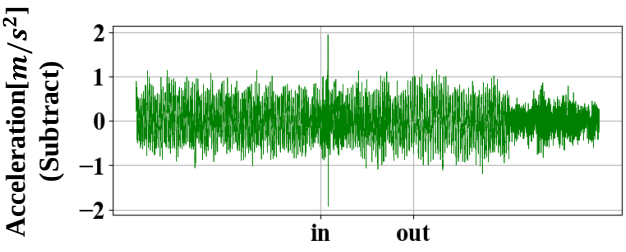

Fig. 8 Subtractions of front and rear vibration measured at a bridge over the A River

ISBN: 978-988-14049-2-3
ISSN: 2078-0958 (Print); ISSN: 2078-0966 (Online)

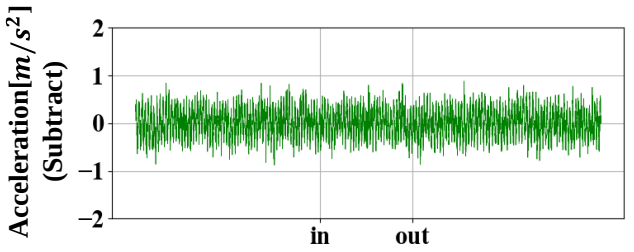

Fig. 9 Subtractions of front and rear vibration measured at a bridge over the P River

In Fig. 7, peaks appeared at both the entry and exit positions. Compared with the results obtained in Fig. 6, it can be seen that the peak amplitude at the position of entry or exit to the bridge is approximately the same. In Fig. 8, a peak can be observed only at the time of penetration. Besides, no peak was observed in Fig. 9. Finally, two of the nine bridges peaked at in and out, and two bridges peaked at either in or out. Although bridges could not observe peaks at many bridges, the bridge response was theoretically included in the difference data. Therefore, it can be assumed that the bridge response could not be visualized because it was affected by other noises. The method of obtaining the difference after the position synchronization corresponds to the processing for removing the road surface unevenness. Therefore, the vehicle response may be visualized if the noise generated by the influence of temperature, wind, bridge damage, etc. other than the road surface irregularity can be removed.

C. The results and discussions of Prediction

We performed supervised learning of binary classification using C-LSTM. 70% of the analysis data were used as learning data and 30% as verification data. The epoch size is 500, and the batch size is 512. Mean Squared Error was used as the loss function, and accuracy was used as the evaluation value. The training data loss after learning was 0.1998, and the correct answer rate was 71.7%. On the other hand, the test data showed a loss of 0.216, and the correct answer was 70.86%. Each bridge was fitted using the learned model. When the predicted value obtained exceeds the threshold value 0.5, 3 of the obtained predicted values giving 1 are shown in Fig. 10. The acceleration data is normalized by Eq (1). Further, it is determined that the predicted value exceeding the threshold σ from Eq (2) exists on the bridge. 0.5 was set in this study.

$$\hat{y} = \begin{cases} 1 & (y \geq \sigma) \\ 0 & (y < \sigma) \end{cases} \tag{2}$$

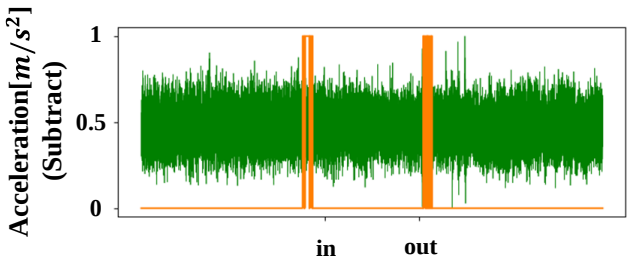

Fig. 10 Subtractions of front and rear vibration measured at a bridge over the F River and prediction result

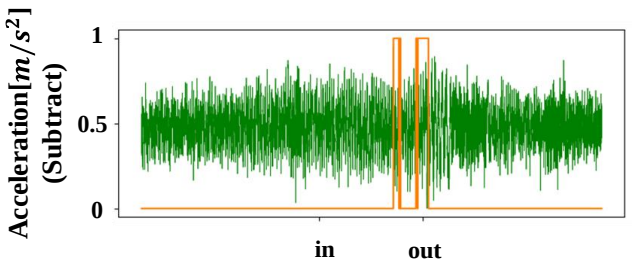

Fig. 11 Subtractions of front and rear vibration measured at a bridge over the S River and prediction result

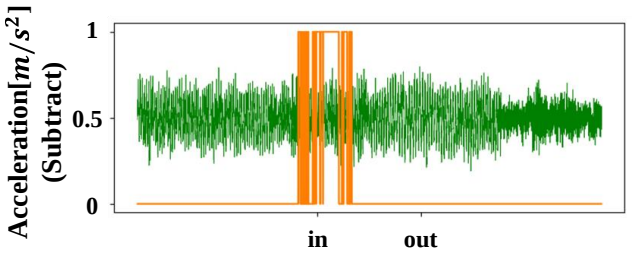

Fig. 12 Subtractions of front and rear vibration measured at a bridge over the B River and prediction result

Although it cannot be said that the accuracy is high, it is possible to specify the bridge position roughly. In this study, the window size was determined to be 1000 regardless of the bridge length. The closer the bridge is to the center, the more it swings. Therefore, the structure learned by C-LSTM may differ depending on the length of the bridge. In order to improve this, it is necessary to change the window size for each bridge. The data used for the analysis is only the data obtained by taking the difference between the front axis and the rear axis under the spring in one trial. A study conducted by Locke et al. [4], which examined the relationship between various noises and bridge damage detection using CNN, combined various data such as vehicle weight, vehicle speed, and time of day. Malekjafarian et al. [11] used 100 measured data to develop bridge damage detection technology using neural networks. These studies may help improve prediction accuracy.

IV. Conclusion

In this study, the verification of the bridge position estimation technique verified in the simulation was carried out in the field experiment. In this study, we focused only on eliminating the effects of road surface irregularities so that noise reduction from temperature, wind, bridge damage, Etc., remains as a research subject. We also performed supervised binary classification for bridge location estimation using C-LSTM. The analytical results showed that it was possible to roughly specify the bridge position, though the accuracy was not high. However, since the window size is constant, the structure learned by C-LSTM may differ depending on the length of the bridge. There are also still issues with the quantity and quality of learning data.

ISBN: 978-988-14049-2-3
ISSN: 2078-0958 (Print); ISSN: 2078-0966 (Online)

REFERENCES

[1] Yang, Y.B., Lin, C.W., and Yau, J.D., "Extracting bridge frequency from the dynamic response of a passing vehicle", *Journal of Sound and Vibration*, vol.272, pp.471-493, 2004.

[2] H. Wang, T. Nagayama, J. Nakasuka, B. Zhao, and D. Su, "Extraction of bridge fundamental frequency from estimated vehicle excitation through a particle filter approach", *Journal of Sound and Vibration*, Vol.428, pp.44-58, 2018.

[3] K. Yamamoto, and Y. Takahashi, "Experimental Validation of Bridge Screening Method based on Vehicle Response Analysis", *Proc. of World Congress on Engineering 2017*, vol.2, pp.928-933, London, U.K., July 5-7, 2017.

[4] Locke, W., Sybrandt, J., Redmond, L., Safro, I., and Atamturktur, S., "Using drive-by health monitoring to detect bridge damage considering environmental and operational effects", *Journal of Sound and Vibration*, vol.468, 115088, 2020.

[5] Murai, R., Miyamoto, R., Yamamoto, K., and Okada, Y., "Numerical Experiments of Bridge Position Estimation for On-Going Monitoring", *Proceedings of the World Congress on Engineering 2019*. pp.474-479, London, U.K., July 3-5, 2019.

[6] Kim, T. Y., and Cho, S. B., "Web traffic anomaly detection using C-LSTM neural networks". *Expert Systems with Applications*, vol.106, pp.66-76, 2018.

[7] Donahue, J., Anne Hendricks, L., Guadarrama, S., Rohrbach, M., Venugopalan, S., Saenko, K., and Darrell, T., "Long-term recurrent convolutional networks for visual recognition and description", *In Proceedings of the IEEE conference on computer vision and pattern recognition*, pp. 2625-2634, 2015.

[8] Kim, T. Y., and Cho, S. B., "Predicting the household power consumption using CNN-LSTM hybrid networks". *In International Conference on Intelligent Data Engineering and Automated Learning*, pp. 481-490, Springer, Cham, 2018.

[9] Zhou, C., Sun, C., Liu, Z., and Lau, F., "A C-LSTM neural network for text classification", arXiv preprint arXiv:1511.08630. 2015.

[10] Jiang, W., Hong, Y., Zhou, B., He, X., and Cheng, C., "A GAN-Based Anomaly Detection Approach for Imbalanced Industrial Time Series", *IEEE Access*, vol.7, 143608-143619. 2019.

[11] Malekjafarian, A., Golpayegani, F., Moloney, C., and Clarke, S., "A machine learning approach to bridge-damage detection using responses measured on a passing vehicle", *Sensors*, vol.19(18), 4035, 2018.

ISBN: 978-988-14049-2-3
ISSN: 2078-0958 (Print); ISSN: 2078-0966 (Online)